The second Born approximation for the ionization of molecules by electron and positron impact

C. Dal Cappello[1], Z. Rezkallah[2], S. Houamer[2], I. Charpentier[3], P.A. Hervieux[4], F. Ruiz-Lopez[5], R. Dey[6] and A. C. Roy[7]

[1]*Université Paul Verlaine-Metz, Laboratoire de Physique Moléculaire et des Collisions, Institut Jean Barriol (FR2843), 1 Boulevard Arago, 57078 Metz Cedex 3, France*

[2]*Laboratoire de Physique quantique et systèmes dynamiques, Département de Physique, Faculté des Sciences Université Ferhat Abbas, Sétif 19000, Algeria*

[3]*Université Paul Verlaine-Metz, Laboratoire d'Etude des microstructures et de Mécanique des Matériaux UMR 7239, ile du Saulcy, 57045 Metz Cedex 1 France*

[4]*Institut de Physique et Chimie des Matériaux de Strasbourg, 23 rue du Loess, BP 43, 67034 Strasbourg Cedex 2 France*

[5]*Nancy-University, Equipe de Chimie et Biochimie théoriques, UMR CNRS-UHP 7565, BP 239, 54506 Vandoeuvre-les–Nancy, France*

[6]*Max-Planck Institut für Plasmaphysik, Boltzmannstr. 2, D-85748 Garching, Germany*

[7]*School of Mathematical Sciences, Ramakrishna Mission Vivekananda University, Belur Math 711202, West Bengal, India*

Abstract

The second Born approximation is applied to study the ionization of molecules. The initial and final states of the target are described by one center wave functions. For the initial state a Gaussian wave function is used while for the ejected electron it is a distorted wave. Results of the present model are compared with recent (e,2e) experiments on the water molecule. Preliminary results are also presented for the ionization of the thymine molecule by electrons and positrons.

PACS: 34.80.Dp

Keywords: single ionization, second Born approximation, ionization of thymine.

Corresponding author: S. HOUAMER

Université Ferhat Abbas

Laboratoire de Physique quantique et systèmes dynamiques, Département de Physique, Faculté des sciences.

Setif 19000, Algeria.

Phone: …… fax …

E-mail : ……..

I INTRODUCTION

Ionization of molecules by light charged particles (electrons and positrons) is a difficult problem and is a true challenge for theoreticians. One of the difficulties is that the molecular states are described by multicenter wave functions. A way to avoid this difficulty is to replace the multicenter wave function by a single center one. For instance, Hafied *et al*. [1] and Dal Cappello *et al*. [2] have been able to overcome this difficulty in their calculations for the water molecule and for the cytosine molecule, respectively. In the first case it was easy because the center of the water molecule was considered to lie at the center of oxygen atom, and a good convergence was reached using only two partial waves, i.e., L=0 and L=1. In the second case the convergence was reached with an increasing number of partial waves , i.e. , with L=0 to L=5 in their study of the ionization of cytosine by protons.

In this paper we extend our first Born model to the next higher second Born model, because the energy of incident electrons used in the recent (e,2e) experiments of Milne-Brownlie *et al*. [3], Kaiser *et al.* [4] and Nixon *et al*. [5] for the ionization of the water molecule is small (from 30 eV to 250 eV). For this energy range one needs the use of theories more appropriate than the first Born approximation. For instance, the lack of symmetry about the momentum transfer in the experimental data demands that the second born approximation is at least necessary. Experiments on the ionization of thymine by electron impact are in progress in the laboratory of Lohmann (see for instance [6]) and are planned to be performed at an incident energy of 250 eV. In this kind of (e,2e) experiments the ejected electron is detected in coincidence with the scattered electron. For the above kinematical arrangement the ejected electrons have low velocities (their energies vary between 10 eV and 20 eV) contrary to those of the scattered electrons (their energies are close to 200 eV). This allows us to ignore the exchange effects.

Up to now, there is no quantum mechanical theory for the ionization of thymine or other DNA bases. Nevertheless total cross sections for the four bases of DNA (adenine, cytosine, guanine and thymine) have been calculated by using semi-classical models. Bernhardt and Paretzke [7] have used the semi-classical Deutsch-Märk formalism (DM) [8] and the Binary-Encounter-Bethe (BEB) theory [9]. These simple models can be applied to determine the electron impact ionization cross sections for various atoms, molecules and ions. They only need molecular structure information which can be provided by the Hartree-Fock method. However, we notice that the BEB and the DM models are not quite successful in describing the last experiments of Shafranyosh et al. [10] for the ionization of the cytosine molecule by electrons. These two models yield a maximum total cross section of 15×10^{-16} cm^2 against 8×10^{-16} cm^2 found in the experiments. Even the more recently improved binary-encountered dipole model (iBED) [11]

gives a maximum total cross section of 17 x 10^{-16} cm^2 [12] although this model perfectly reproduces the total cross section of the water molecule [12]. The iBED model differs from the BEB model in two main aspects. First, the iBED treatment takes into account the long-range electron-target dipole interaction (as in the BEB model) in addition to the shielding of the dipole field as the scattering electron comes inside the bonding region. Secondly, this model predicts an $(E_e)^{-3.5}$ ejected electron energy dependence instead of $(E_e)^{-3}$ as in the BEB model for the optical oscillator strength.

It is worth stressing that all these models (DM, BEB and iBED) are unable to calculate triple differential cross sections (TDCS) which are measured in (e,2e) experiments. To date the most accurate model to calculate the TDCS is the molecular three-body distorted-wave approach (M3DW) [13-14] which is a generalization of the three-body distorted-wave approximation (3DW) [15] for molecules. In the 3DW any interaction included in the calculation of both the initial state and the final state is contained to all orders of perturbation theory while all interactions contained in the perturbation operator are of first-order in perturbation theory. As the TDCS depends on molecular orientation, the usual (e,2e) measurements provide an average over all molecular orientations. However, the M3DW model needs a lot of computer time and Gao *et al.* [13] proposed the orientation-averaged molecular orbital (OAMO) where a single average molecular orbital is used to approximate the average over all orientations. This approximation is only successful for a *few* highly symmetric states. For instance, this approximation is not valid for the $1b_1$ state of the water molecule [14]. For the case of the ionization of the water molecule other less sophisticated models were applied. Champion *et al.* [16] used the distorted wave Born approximation (DWBA) where the incident and scattered electrons are described by plane waves while the ejected electron is described by a distorted wave. But this model was unable to reproduce the recoil peak in the experiments of Milne-Brownlie *et al.* [3] because Champion *et al.* [16] neglected the interaction between the incident electron and the nucleus of the target. When this last interaction was included in the DWBA model a better agreement was found [17]. Champion et al. [17] also introduced the well-known BBK model [18] where all the interactions have been taken into account: the interaction of the ionized target with the projectile electron as well as the ejected electron and the repulsion between the outgoing electrons. In this BBK model the scattered electron and the ejected electron are described by a Coulomb wave while in the M3DW model distorted waves are used.

In this paper we decide to use the second Born approximation which is more tractable than the BBK model for complex molecules like DNA bases. The ionization of such a molecule is important for life science because it is now known [19] that low energy secondary electrons

(less than 20 eV) strongly interact with biological molecules in the DNA via dissociative electron attachment [20]. These interactions lead to single or double DNA strand breakage.

In Section II we present our theoretical model to describe the ionization of a molecule by electrons or positrons. Then, in Section III, the TDCS results are compared with experimental data for the ionization of water. We also present preliminary results for the ionization of thymine. Finally, conclusions about the modelling of the ionization of molecules by electrons and positrons are outlined in section IV.

Atomic units are used throughout unless otherwise indicated.

II THEORY

The ionization of a molecule M by an electron (or a positron) can be considered as a pure electronic transition since the closure relation over all possible rotational and vibrational states of the residual target can be applied. This is justified by the values of the collision time compared to the characteristic time of rotation and vibration. The exchange effects will be neglected since the scattered electron is much faster than the ejected one in all the cases considered here.

The single ionization of a molecule M by an electron is written as:

$$M + e^- \longrightarrow M^+ + e^- + e^- \qquad (1)$$

In the second Born approximation (SBA), the four-fold differential cross section (4DCS) is written, for a given molecular orientation defined by the Euler angles $(\alpha;\beta;\gamma)$, as

$$\sigma^{(4)}(\alpha;\beta;\gamma) = \frac{d^4\sigma(\alpha;\beta;\gamma)}{d\Omega_{Euler}\, d\Omega_s\, d\Omega_e\, dE_e} = \frac{k_s k_e}{k_i}\left| f_{B1} + f_{B2}\right|^2, \qquad (2)$$

where $d\Omega_{Euler} = \sin\beta d\beta d\alpha d\gamma$ and $d\Omega_s$ and $d\Omega_e$ denote the elements of solid angles for the scattered and the ejected electron, respectively, whereas the energy interval of the ejected electron is represented by dE_e. The momenta of the incident, the scattered, and the ejected electrons are denoted by $\vec{k}_i$, $\vec{k}_s$, and $\vec{k}_e$, respectively.

In an (*e*,2*e*) reaction the conservation of energy imposes: $\frac{k_i^2}{2} = \frac{k_s^2}{2} + \frac{k_e^2}{2} + I_i$ where I_i represents the energy needed to eject one electron from the molecule.

The first Born term f_{B1} is written as

$$f_{B1} = -\frac{1}{2\pi}\left\langle \exp(i\vec{k}_s.\vec{r}_0)\Psi_f(\vec{k}_e,\vec{r}_1,..,\vec{r}_n)\middle|V\middle|\exp(i\vec{k}_i.\vec{r}_0)\Phi_i(\vec{r}_1,..,\vec{r}_n)\right\rangle, \quad (3)$$

where $\Phi_i(\vec{r}_1,..,\vec{r}_n)$ is the wave function of the initial state of the molecule while $\Psi_f(\vec{k}_e,\vec{r}_1,..,\vec{r}_n)$ represents the wave function for the single continuum state of the molecule.

In Eq.(3), the potential *V* represents the Coulomb interaction between the incoming electron and the target and is written as

$$V = -\frac{Z}{r_0} - \sum_{j=1}^{N} \frac{1}{\left|\vec{r}_0 - \vec{R}_j\right|} + \sum_{i=1}^{n} \frac{1}{\left|\vec{r}_0 - \vec{r}_i\right|}, \quad (4)$$

where $\vec{r}_i$ is the position vector of the i^{th} bound electron of the target with respect to the centre of the molecule, $\vec{r}_0$ denotes the coordinate of the incident particle and $\vec{R}_j$ is the position of the jth nucleus.

The second Born term f_{B2} is given by

$$f_{B2} = \frac{1}{8\pi^4}\sum_m \int \frac{d\vec{q}}{q^2 - k_m^2 - i\varepsilon} \times \left\langle \exp(i\vec{k}_s.\vec{r}_0)\Psi_f(\vec{k}_e,\vec{r}_1,..,\vec{r}_n)\middle|V\middle|\exp(i\vec{q}.\vec{r}_0)\Phi_m(\vec{r}_1,..\vec{r}_n)\right\rangle \times \left\langle \exp(i\vec{q}.\vec{r}_0)\Phi_m(\vec{r}_1,..\vec{r}_n)\middle|V\middle|\exp(i\vec{k}_i.\vec{r}_0)\Phi_i(\vec{r}_1,..\vec{r}_n)\right\rangle \quad (5)$$

where the summation over *m* means that we take into account all the contributions of the *m* discrete and continuum states of the molecule, $\Phi_m(\vec{r}_1,..\vec{r}_n)$ being the wave function for a discrete or continuum state of the molecule. It means that the incident electron collides two times with the target.

The reduction of this difficult n-electron target problem to a single electron target may be done within the well-known frozen-core approximation. In this case this target electron will be ejected during the single ionization process. Moreover, it is worthwhile to note that the electrons in the singly charged ion core are assumed to remain unaffected by the ionization process. This is a reasonable approximation provided that our study is limited to the ejection of valence shell electrons.

Note that the integration over the projectile coordinates (r_0) can be performed analytically so that the second Born term, by applying the closure approximation [21], becomes:

$$\bar{f}_{B2} = \frac{2}{\pi^2}\int \frac{d\vec{q}}{q^2 - p^2 - i\varepsilon}\frac{1}{K_i^2 K_f^2} \left\langle \Psi_C^-(\vec{k}_e, \vec{r}_1)\left|\exp(i\vec{K}_f.\vec{r}_1) - 1\right|\exp(i\vec{K}_i.\vec{r}_1) - 1\left|\Phi_i(\vec{r}_1)\right.\right\rangle \tag{6}$$

where $\vec{K}_i = \vec{k}_i - \vec{q}$ and $\vec{K}_f = \vec{q} - \vec{k}_s$, and $\vec{K} = \vec{K}_i + \vec{K}_f = \vec{k}_i - \vec{k}_s$ is the momentum transfer.

We have also

$$\frac{p^2}{2} = \frac{k_i^2}{2} - \overline{w}\,, \tag{7}$$

where $\overline{w}$ refers to the average excitation energy. In our study we have $\overline{w} = I_i$ which corresponds to the usual choice for the single ionization of an atom or a molecule [28].

When we consider a single electron target it is also possible to apply the eikonal approximation (EA) [22]. This approximation is valid for small momentum transfer to the target and sufficiently high incident energy [23]. The 4DCS in the eikonal approximation [23] is given by:

$$\sigma^{(4)}(\alpha;\beta;\gamma) = \frac{d^4\sigma(\alpha;\beta;\gamma)}{d\Omega_{Euler}\,d\Omega_s\,d\Omega_e\,dE_e} = \frac{k_s k_e}{k_i}\left|T_{fi}\right|^2, \tag{8}$$

where

$$T_{fi} = -\frac{1}{2\pi}\left\langle \exp(i\vec{k}_s.\vec{r}_0)\Psi_C^-(\vec{k}_e, \vec{r}_1)\left|\frac{1}{r_{01}} - \frac{1}{r_0}\right|\exp(i\vec{k}_i.\vec{r}_0)\Phi_i(\vec{r}_1)\right\rangle \times\left[\frac{r_{01} - \vec{r}_{01}.\hat{z}}{r_1 - \vec{r}_1.\hat{z}}\right]^{i/k_i}, \tag{9}$$

with $\hat{z} = \frac{\vec{k}_i}{k_i}$. In contrast to the first Born approximation (FBA), EA which has been applied with success to a wide variety of atomic collisions including elastic scattering, excitation and ionization has contributions from projectile-target nucleus interaction and multiple scattering effects. In fact, the eikonal amplitude contains terms of all orders in V (i.e., the sum of the projectile-nucleus interaction and the projectile-bound electron interaction) in its phase in an approximate way.

The water and thymine wave functions have been obtained using the Gaussian 03 program [24] as follows. In the case of water, the wave function has been computed at the Hartree-Fock level of theory using the augmented, correlation-consistent, polarized-valence quadruple-zeta basis set (aug-cc-pvQZ) employed in our previous work [1]. Geometry optimization has been done including electronic correlation energy at the second-order Moller-Plesset perturbation theory (MP2). For thymine, we have chosen a lower computational level that we previously used for cytosine [2]. The geometry of the molecule has also been optimized at the MP2 level but using now the 6-31G(d) basis set that includes a double-zeta valence shell and polarization orbitals on non-hydrogen atoms. The molecular orbitals hereafter correspond to the Hartree-Fock calculations. The multicenter wave function is then converted to a single-center expansion (see appendix) of usual Slater-type functions by using partial-wave expansion techniques [1, 25].

Here we restrict here this study to the valence electrons because inner shell electrons need many partial waves for the expansion.

All the one-center molecular wave functions $\Phi_i(\vec{r})$ (with i ranging from 1 to 48 for the thymine), containing the valence electrons, can be expressed by linear combinations of Slater-type functions and are written as

$$\Phi_i(\vec{r}) = \sum_{k=1}^{N_i} a_{ik} \phi_{n_{ik} l_{ik} m_{ik}}^{\varepsilon_{ik}}(\vec{r}), \qquad (10)$$

where N_i is the number of Slater functions used in the construction of the j^{th} molecular orbital and a_{ik} the weight of each *complex* atomic component $\phi_{n_{ik} l_{ik} m_{ik}}^{\varepsilon_{ik}}(\vec{r})$.

In Eq. (10), $\phi_{n_{ik}l_{ik}m_{ik}}^{\varepsilon_{ik}}(\vec{r})$ is written as

$$\phi_{n_{ik}l_{ik}m_{ik}}^{\varepsilon_{ik}}(\vec{r}) = \left(R_{n_{ik}}^{\xi_{ik}}(r) + iS_{n_{ik}}^{\xi_{ik}}(r)\right)Y_{l_{ik}}^{m_{ik}}(\hat{r}), \tag{11}$$

where the radial part $\left(R_{n_{ik}}^{\xi_{ik}}(r) + iS_{n_{ik}}^{\xi_{ik}}(r)\right)$ can be given by the usual radial Slater–type functions such as $b_{n_{ik}} r^{n_{ik}-1}\exp(-\varepsilon_{ik} r)$.

We notice that here the generated wave function is generally *complex* whereas it was real in the case of Moccia' wave functions [26].

In our present model the scattered electron is described by a plane wave, whereas the ejected electron can be described by a distorted wave or a Coulomb wave. Owing to the prohibitively long time needed for the calculation of the second Born term we only use a Coulomb wave for the ejected electron:

$$\begin{aligned}\varphi_C(\vec{k}_e,\vec{r}_1) = &\frac{\exp(i\vec{k}_e.\vec{r}_1)}{(2\pi)^{3/2}}{}_1F_1(-iZ_e/k_e,1,-i(\vec{k}_e.\vec{r}_1 + k_e r_1)) \\ &\times \exp(\frac{\pi Z_e}{2k_e})\Gamma(1+iZ_e/k_e).\end{aligned} \tag{12}$$

The effective ionic charge Z_e is taken to be equal to 1 (Brothers and Bonham [27]).

For the positron impact the only change in our model is to write *V* as:

$$V = \frac{Z}{r_0} + \sum_{j=1}^{N}\frac{1}{\left|\vec{r}_0 - \vec{R}_j\right|} - \sum_{i=1}^{n}\frac{1}{\left|\vec{r}_0 - \vec{r}_i\right|}, \tag{13}$$

Under these conditions, it is clear that exactly same 4DCS will be obtained for electrons and positrons when the single ionization process is described within the 1st Born approximation. On the contrary, when the second term of Born series is used, differences will appear between electron and positron 4DCSs since the sign of the second Born term does not depend on the charge of the particle. Finally, it is important to note that in the second Born term the integrals over $d\vec{q}$ must be performed numerically with a great care [28] since the integrand is singular at $q = k_m$ (equation (5)) or $q = p$ (equation (6)).

The wave functions $\Phi_i(\vec{r})$ correspond to a particular orientation of the molecular target given by the Euler angles (α, β, γ) [29, 30]. Thus, the four differential cross sections we have calculated with Eq. 2 through Eq. 10 correspond to the ionization of an oriented molecule. Under these conditions, we need to average these differential cross sections in order to compare with experiment. The averaging is accomplished by an analytical integration over the Euler angles, owing to the property of the rotation matrix [17, 29, 30].

$$\frac{1}{8\pi^2}\int d\Omega D^{l}_{\mu,m}(\alpha,\beta,\gamma)D^{l'^{*}}_{\mu',m'}(\alpha,\beta,\gamma) = \frac{1}{2l+1}\delta_{l,l'}\delta_{m,m'}\delta_{\mu,\mu'}\ , \qquad (14)$$

where $D^{l}_{\mu,m}(\alpha,\beta,\gamma)$ represents the rotation matrix with $Y^{l}_{m}(\hat{r}) = \sum_{\mu=-l}^{l} D^{l}_{\mu,m}(\alpha,\beta,\gamma)Y^{l}_{\mu}(\hat{r})$ for the transformation of the molecular orientation from the molecular frame to the laboratory frame. Eq. 14 can also be applied to our models including the second Born approximation with the closure approximation (Eq. 6) as for other sophisticated models as the CDW-EIS approximation [31-32] or BBK [17]. These two models (CDW-EIS and BBK) need a six-dimensional integral.

In general, the DWBA model gives reasonable agreement with the TDCS measurements for electron-impact ionization of atoms and molecules if the incident electron has an energy of about 100 eV or larger [14].

III RESULTS AND DISCUSSION

Our model is first applied to the ionization of the water molecule. Recently (e,2e) experiments were performed by Milne-Brownlie et al. [3] for the $2a_1$ state, the $1b_1$ state, the $1b_2$ state and the summed $3a_1$+$1b_1$ states for 250 eV incident particles and slow ejected electrons (8 eV and 10 eV). Kaiser et al. [4] reported results only for the $1b_1$ state at incident electron energies varying between 30 eV and 110 eV. Nixon et al. [5] were able to measure TDCS for the $3a_1$ state at low energies (from 4 eV to 40 eV above threshold). We restrict our present study to the higher incident energy (250 eV) where several models have been applied. The DWBA model of Champion et al. [3, 16] was able to reproduce the binary peak but not the recoil structure experimentally observed. When the interaction between the incident electron and the target nucleus was taken into account the agreement was better [17] but some discrepancies still remained. Finally, when the BBK [17-18] and the DS3C model (BBK with effective charges) [17, 33-34] had been applied, the agreement improved particularly for the ionization of the $2a_1$ state. These models were applied using the one center wave function of Moccia [26]. Our aim

is to show that the present models (Eikonal Approximation and second Born approximation) are also able to predict TDCS in good agreement with experiment. All the TDCSs are given in atomic units.

The figures 1a and 1b show that the partial wave expansion of the multicenter wave function corresponding to the initial state $2a_1$ is simply reduced to L=0, the other terms (L=1 to L=5) being negligible. It is interesting to notice that the wave function of Moccia for the initial state $2a_1$ is mainly built of L=0 too. Figure 2a shows the results of the first and second Born approximations together with those of the eikonal approximation. The shift of the binary peak is well reproduced by our second Born approximation. The eikonal approximation without the post collisional effect (PCI) is not able to reproduce such a shift. Compared to the BBK or DS3C models our models including the second Born approximation or the eikonal approximation slightly underestimate the magnitude of the recoil peak. Figure 2b presents an interesting comparison between the TDCS obtained for the electron impact and for the positron impact. As in the case of the ionization of the atomic hydrogen [18, 28] we find that the magnitude of the binary peak increases for the positron impact while that of the recoil peak decreases.

Figure 3a shows the summed TDCS of our second Born approximation for the ionization of the sum of the two states $3a_1$ and $1b_1$. We find good agreement between our model and the data of Milne-Brownlie *et al*. [3]. We notice that the symmetry around the momentum transfer is destroyed and that a double lobe of the binary peak appears. The magnitude of the second peak increases while that for the first peak decreases. This is admittedly a typical characteristic feature of the second Born approximation for the p orbital. In the present case, both the $3a_1$ and the $1b_1$ are mainly dealt with the L=1 partial wave expansion. When we consider the ionization of the two states $3a_1$+$1b_1$ by positrons (Figure 3b) we see a complete change in the structure of the binary peak: the first peak increases while the second peak decreases. We notice that the recoil peak decreases too. Due to a lot of parametric differentiations [35] the eikonal approximation is not applied for the ionization of the $1b_1$, $1b_2$ and $3a_1$ states .

Figure 4a for the ionization of the $1b_1$ state by electrons gives the same pattern as in Figure 3a. We nevertheless see that the agreement with experiment is a little bit less good in the small-ejected angle region. Figure 4b displays a comparison of the TDCS for the $1b_1$ state obtained in the FBA and SBA for electron and positron impact. Here we also observe that the first peak of the binary peak increases while the second peak decreases for the positron impact.

Figure 5a shows the results for the ionization of the $1b_2$ state by electron impact. The SBA results are in better agreement with the experimental data of Milne-Brownlie *et al*. [3] than the FBA. Figure 5b for the electron and positron impact shows the same results as in figures 3b

and 4b: the symmetrical double-peak structure of the binary peak given by the first Born approximation is destroyed when the second Born approximation is applied. This result was also obtained with the BBK and DS3C models [17]. As a matter of fact, the three states ($3a_1$, $1b_1$ and $1b_2$) are mainly built by the L=1 partial wave expansion of the initial state of the wave function. We also observe that our second Born model with the closure approximation practically reproduces the same results as those given by the BBK or DS3C models. The agreement between these models and the experimental data [3] is very good. This good agreement is found in the vicinity of the Bethe ridge [36]. In this case the momentum transfer is close to the value of the momentum of the ejected electron $K \approx k_e$.

We now investigate the ionization of the thymine molecule which is planned to be studied in the near future by the experimental group of Lohmann [6]. Thymine has 66 electrons but our model can only be applied for the 48 electrons of the valence shells. For the remaining 18 electrons of the inner shells the convergence of our single-center expansion compared to the multicenter wave function is very slow. In this paper we investigate the ionization of the last four shells for which the ionization potentials are estimated to be 9.14 eV, 11 eV, 11.4 eV and 12.16 eV respectively [7]. The experimental conditions are the following: the incident energy is E_i=250 eV and the energy of the ejected electron is E_e=20 eV while the geometrical conditions are given by $\varphi_s = 180^0$, $\varphi_e = 0^0$ and $\theta_s = 15^0$ or $\theta_s = 10^0$. The choice of $\theta_s = 15^0$ practically corresponds to the Bethe ridge.

Next we check the convergence of our partial wave expansion of the multicenter wave function by applying the first Born approximation for $\theta_s = 15^0$ and for the last valence shell (I_i=9.14eV). Figures 6a and 6b clearly show that the convergence is reached at L=8 (from L=1 to L=8). In the figures 6 we see a double-peak structure for the binary peak as in the cases of the ionization of the water molecule ($3a_1$, $1b_1$ and $1b_2$ states). When we change the scattering angle ($\theta_s = 10^0$), figures 7a and 7b give the same curves as those in the previous case ($\theta_s = 15^0$) except the magnitude which increases here. The convergence of our partial wave expansion is reached at L=8 too. Another interesting fact is the small magnitude of the recoil peak contrary to the case of the ionization of water. It is certainly due to the higher value of the energy of the ejected electron here (20 eV instead of 8 eV or 10 eV) because, generally speaking, the magnitude of the recoil peak increases when the energy of the ejected electron decreases. The results are very similar in the case of the ionization of the second outer shell (I_i=11eV). The convergence is again reached at L=8 in the two cases ($\theta_s = 15^0$ or $\theta_s = 10^0$)

and the magnitudes are very close (figures 8 and 9). More interesting is the case of the third outer shell (I_i=11.4eV). We observe a complete change in the shapes of the curves when we consider $\theta_s = 15^0$ (figures 10a and 10b) and $\theta_s = 10^0$ (figures 11a and 11b). In the first case ($\theta_s = 15^0$) we get a minimum in the direction of the momentum transfer (binary peak) while we get a plateau in the second case $\theta_s = 10^0$. The convergence is reached for L=9 (from L=0 to L=9). More exciting are the results for the ionization of the fourth outer shell (I_i=12.16 eV). A rich complex structure is observed for the binary peak (four peaks) in the figures 12 ($\theta_s = 15^0$) while we have only a single peak for $\theta_s = 10^0$ (figures 13). The convergence is reached at L=8 for the binary peak but the recoil peak needs more terms (from L=0 to L=15).

From the above analysis it seems very interesting to study the third and fourth outer shells which exhibit very complex structures for the binary peak in the Bethe ridge ($\theta_s = 15^0$). This complex structure disappears for $\theta_s = 10^0$.

The second Born approximation requires a large amount of computer time. Typically the second Born approximation for the ionization of the water molecule needs 6 hours for one point while for the thymine molecule it is around 40 days. So we present only one figure for the ionization of the first valence orbital of the thymine by electron and positron impacts. In figure 14 we notice that the symmetry around the momentum transfer is destroyed and that a double lobe of the binary peak appears. As in the case of the ionization of water the magnitude of the second peak increases for the electron impact. When we consider the ionization by positrons we see a change in the structure of the binary peak: the first peak increases.

IV CONCLUSION

Triple differential cross sections for the ionization of water and thymine molecules obtained in the second Born and eikonal approximation methods are presented and discussed. Our models use single center wave functions and provide results in good agreement with other models (BBK and DS3C) and with the experimental data of Milne-Brownlie et al. [3] for the ionization of the water molecule. In this case the convergence of our partial wave expansion of the initial multicenter wave function is very fast and limited to one term (L=0 or L=1). In the case of thymine the ionization of the four last outer shells needs more terms in the expansion of the initial wave function (generally up to L=8 or L=9). We observe in some cases a rich complex structure in the curves in the Bethe ridge. All these results can now be an impetus for the future

experiments about the ionization of the thymine molecule by electrons. We also study the ionization of water and thymine molecules by positrons. When we compare the present cross sections with the results given by the first Born approximation it is observed that the magnitude of the recoil peak decreases while that of the binary peak increases.

We hope that this work opens the way to new experiments, especially for triple differential cross sections which give the most accurate information about the mechanism of the ionization of an atom or a molecule. A knowledge of this mechanism is essential for the study of the penetration of charged particles through biological matter.

ACKNOWLEDGMENTS

We would like to thank the PMMS (Pôle Messin de Modélisation et de Simulation) for computer time.

APPENDIX

In *ab initio* calculations of molecular electronic structure, the functions which are almost universally used by quantum chemists are the so-called contracted Gaussian-Type Orbitals (cGTOs), more specifically contracted Cartesian Gaussian-Type Orbitals (cCGTOs) of the form

$$\varphi_i = \sum_{j=1}^{n_p} d_{ij} \chi_j \ , \qquad \text{A1}$$

where the coefficients d_{ij} are the contraction coefficients and the functions χ_j are the *primitive* Cartesian Gaussian-Type Orbitals (CGTOs) called also Cartesian Gaussian. Generally the number of CGTOs varies between 1 and 7 (*i.e.* $1 \le n_p \le 7$). These functions are defined as

$$\chi_a(x,y,z) = N_{\alpha,i,j,k}(x-x_A)^i (y-y_A)^j (z-z_A)^k \exp(-\alpha\left|\vec{r}-\vec{R}_A\right|^2), \qquad \text{A2}$$

where a denotes the parameter set $a = (\alpha, \vec{R}_A, i, j, k)$, $\vec{r} = (x,y,z)$, $\vec{R}_A = (x_A, y_A, z_A)$ and $N_{\alpha,i,j,k}$ is a normalization constant such as

$$N_{\alpha,i,j,k} = \left(\frac{2\alpha}{\pi}\right)^{3/4} \left(\frac{2^{2(i+j+k)}\alpha^{i+j+k}}{(2i-1)!!(2j-1)!!(2k-1)!!}\right)^{1/2} . \qquad \text{A3}$$

In the above expression the following definition is used: $(2n)!! = 2.4.6..(2n)$, $(2n+1)!! = 1.3.5..(2n+1)$ and $0!! = (-1)!! = 1!! = 1$. The parameter α controls the width of the orbital (a large (small) value gives a tight (diffuse) function) and i, j, k, control the angular momentum, $l = i + j + k$. Generally, quantum chemistry calculations are restricted to $l \leq 4$ (*i.e.* g-orbitals). Here Φ_i denotes a molecular orbital (*e.g.* $1b_1$ of the water molecule) and is defined by

$$\Phi_i(x, y, z) = \sum_{k=1}^{n_c} a_{ik} \varphi_k \qquad \text{A4}$$

where n_c is the number of cCGTOs which is of the order of few hundred. The coefficients a_{ik} are obtained from the program Gaussian 03.

A Spherical Gaussian Type Orbital (SGTO) is defined as

$$\phi_b(\vec{r}) = N_{\alpha,n,l} \left| \vec{r} - \vec{R}_A \right|^{2n+l} Y_{l,m}(\Omega_{\vec{r}-\vec{R}_A}) \exp(-\alpha \left| \vec{r} - \vec{R}_A \right|^2), \qquad \text{A5}$$

with $b = (\alpha, \vec{R}_A, n, l, m)$, and

$$N_{\alpha,n,l} = \left(2 \frac{(2\alpha)^{2n+l+3/2}}{\Gamma(2n+l+3/2)} \right)^{1/2} \qquad \text{A6}$$

a normalization constant.

The functions χ_a defined in A2 and ϕ_b defined in A5 are linked together through the transformation

$$\chi_a(x, y, z) = \sum_{n,l,m} A(ijk; nlm) \phi_b(\vec{r}), \qquad \text{A7}$$

where the summation is restricted by the condition $2n + l = i + j + k$.

Most of the computer programs in the field of atomic and molecular collisions use the partial wave expansion techniques. It means that the molecular wave functions must be expanded around a common center as follows

$$\Phi_i(\vec{r}) = \sum_{\lambda, m_\lambda} \widetilde{R}^i_{\lambda, m_\lambda}(r) Y_{\lambda m_\lambda}(\Omega_{\vec{r}}). \qquad \text{A8}$$

The molecular orbitals coming out from a quantum chemistry program (such as Gaussian 03) are expressed in terms of linear combination of cCGTOs (φ_k in A4) which are themselves linear combination of CGTOs (χ_j in A1). As we have seen previously these latter functions can be expressed in terms of SGTOs (ϕ_b in A7) therefore the expansion A8 can be obtained by performing a single-center expansion of the SGTOs. Following [25, 37] we have

$$\phi_b(\vec{r}) = \sum_{l'=0}^{l_{\max}+l} \sum_{m'=-l'}^{l'} R_{l',m'}(r) Y_{l',m'}(\Omega_{\vec{r}}), \qquad \text{A9}$$

or more explicitly

$$\begin{aligned} &\phi_b(\vec{r}) = 4\pi N_{\alpha,n,l} R_A^{2n} \exp(-\alpha(r^2 + R_A^2)) \\ &\sum_{l_1,l_2=0}^{l} \sum_{\tilde{l}=0}^{\tilde{l}_{\max}} \sum_{l',l''} \sum_{m',m''} C(l_1,l_2,\tilde{l},l',m',l'',m'',l,m) r^{l_1} R_A^{l_2} \varsigma_{\tilde{l}}^{2n}(\alpha,r,R_A) \qquad \text{A10} \\ &Y_{l''m''}(\Omega_{\vec{R}_A}) Y_{l'm'}(\Omega_{\vec{r}}) \end{aligned}$$

with

$$\begin{aligned} &C(l_1,l_2,\tilde{l},l',m',l'',m'',l,m) = (-1)^{l+\tilde{l}+m} \delta_{l_1+l_2,l} G(l_1,l_2,l) H(l_1,\tilde{l},l') \\ &H(l_2,\tilde{l},l'') \sqrt{(2l+1)(2l'+1)(2l''+1)} \begin{pmatrix} l' & l'' & l \\ m' & m'' & -m \end{pmatrix} \begin{Bmatrix} l' & l'' & l \\ l_2 & l_1 & \tilde{l} \end{Bmatrix} \end{aligned} \qquad \text{A11}$$

and

$$G(l_1,l_2,l) = (-1)^{l_2} \left(\frac{4\pi(2l+1)!}{(2l_1+1)!(2l_2+1)!} \right)^{1/2}, \qquad \text{A12}$$

and

$$H(l_1,\tilde{l},l') = \left(\frac{(2l_1+1)(2\tilde{l}+1)}{4\pi(2l'+1)} \right)^{1/2} \left\langle l_1 \tilde{l}\, 00 \middle| l'\, 0 \right\rangle, \qquad \text{A13}$$

where $\left\langle l_1 \tilde{l}\, 00 \middle| l'\, 0 \right\rangle$ is a Clebsch-Gordan coefficient.

Moreover

$$\varsigma_{\tilde{l}}^{2n}(\alpha,r,R_A) = 4\pi \sum_{l''=0}^{n} \sum_{l'=|\tilde{l}-l''|}^{\tilde{l}+l''} H^2(l',l'',\tilde{l}) R_{l''}^{2n}(r,R_A) i_{l'}(2\alpha r R_A) \qquad \text{A14}$$

with

$$R_{l''}^{2n}(r,R_A)=\sum_{i=l''}^{2n-l''} T_{l'',i}^{2n}\left(\frac{r}{R_A}\right)^i , \qquad \text{A15}$$

and

$$T_{l'',i}^{2n}=(-1)^{l''}\frac{(2n+1)!}{(i-l'')!!(i+l''+1)!!(2n-i-l'')!!(2n-i+l''+1)!!} . \qquad \text{A16}$$

In the above equation the summation is performed in steps of 2. In the equation A14 the functions $i_l(r)$ are the modified spherical Bessel functions [38] defined as

$$i_l(r)=\sqrt{\frac{\pi}{2r}}I_{l+1/2}(r) , \qquad \text{A17}$$

The presence of the 3j and 6j symbols in A11 and the Clebsch-Gordan coefficient in A13 leads to the following selection rules $\left|\tilde{l}-l_1\right|\le l'\le\tilde{l}+l_1$, $\left|\tilde{l}-l_2\right|\le l''\le\tilde{l}+l_2$, $-l'\le m'\le l'$ and $-l''\le m''\le l''$. The value of $\tilde{l}_{\max}$ is chosen in order to ensure the convergence of A10. Typically, $\tilde{l}_{\max}\approx 10$ is required for not too large molecules such as water.

REFERENCES

[1] H. Hafied, A. Eschenbrenner, C. Champion, M.F. Ruiz-Lopez, C. Dal Cappello, I. Charpentier, and P.A. Hervieux, Chem. Phys. Lett. **439**, 55 (2007).

[2] C. Dal Cappello, P.A. Hervieux, I. Charpentier, and F. Ruiz-Lopez Phys Rev A **78,** 042702 (2008).

[3] D. S. Milne-Brownlie, S. J. Cavanagh, B. Lohmann, C. Champion, P.-A. Hervieux, and J. Hanssen, Phys. Rev. A **69**, 032701 (2004).

[4] C. Kaiser, D. Spieker, J. Gao, M. Hussey, A. J. Murray, and D. H. Madison, J. Phys. B. **40**, 2563 (2007).

[5] K. L. Nixon, A. J. Murray, O. Al-Hagan, D. H. Madison, and C. Ning, J. Phys. B. **43**, 035201 (2010).

[6] C. J. Colyer, S. M. Bellm, F. Blanco, G. Garcia, and B. Lohmann, J. Phys.: Conf. Ser. **288**, 012014 (2011).

[7] Ph. Bernhardt and H. G. Paretzke, Int. J. Mass Spectrom. **223**, 599 (2003).

[8] H. Deutsch, K. Becker, S. Matt, and T. D. Märk, Int. J. Mass Spectrom. **223**, 599 (2003).

[9] Y. K. Kim, M.E. Rudd, Phys. Rev. A **50,** 3954 (1994).

[10] I. Shafranyosh, M.I. Sukhoviya, and M. I. Shafranyosh, J. Phys. B. **39,** 4155 (2006).

[11] W. M. Huo, Phys Rev A **64,** 042719 (2001).

[12] W.M. Huo, C. E. Dateo, and G. D. Fletcher, Radiat. Measurements **41**, 1202 (2006).

[13] J. Gao, D. H. Madison, and J. L. Peacher, J. Chem. Phys. **123**, 204314 (2005).

[14] D. H. Madison and O. Al-Hagan, J. At. Mol. Phys. **2010**, 367180 (2010).

[15] A. Prideaux and D. H. Madison, Phys. Rev. A **67**, 052710 (2003).

[16] C. Champion, J. Hanssen, and P.-A. Hervieux, Phys. Rev. A **65**, 022710 (2002).

[17] C. Champion, C. Dal Cappello, S. Houamer, and A. Mansouri, Phys. Rev. A **73**, 012717 (2006).

[18] M. Brauner, J. S. Briggs, and H. Klar, J. Phys. B. **22**, 2265 (1989).

[19] V. Cobut, Y. Frongillo, J. P. Patau, T. Goulet, M. J. Frazer, and J. P. Jay-Gerin, Radiat. Phys. Chem. **51**, 229 (1998).

[20] B. Boudaïffa, P. Cloutier, D. Hunting, M. A. Huels, and L. Sanche, Science **287**, 1658 (2000).

[21] F. W. Byron Jr and C. J. Joachain Phys. Rev. **146,** 1 (1966).

[22] R. J. Glauber, in *Lectures in Theoretical Physics*, edited by W. E. Brittin and L. G. Dunham (interscience, New York, 1959), Vol. 1, p. 315.

[23] R. Dey and A. C. Roy, NIMB **243**, 28 (2006) and references therein.

[24] M. J. Frisch *et al*., Gaussian 03, Revision B.05, Gaussian, Inc., Wallingford CT, (2004).

[25] K. Kaufmann, W. Baumeister and M. Jungen, J. Phys. B **22**, 2223 (1989).

[26] R. Moccia, J. Chem. Phys. **40,** 2186 (1964).

[27] M. J. Brothers and R. A. Bonham, J. Phys. B **17**, 4235 (1984).

[28] C. Dal Cappello, A. Haddadou, F. Menas, and A. C. Roy, J. Phys. B. **44,** 015204 (2011).

[29] C. Champion, J. Hanssen and P. A. Hervieux, Phys. Rev. A **63,** 052720 (2001).

[30] C. Champion, J. Hanssen and P.A. Hervieux, J. Chem. Phys. **121,** 9423 (2004).

[31] D. S. F. Crothers and J. F. McCann, J. Phys. B **16**, 3229 (1983).

[32] S. Jones and D. H. Madison, Phys. Rev. Lett. **81,** 2886 (1998).

[33] J. Berakdar and J. S. Briggs, Phys. Rev. Lett. **72,** 3799 (1994).

[34] S. Zhang, J. Phys. B. **33,** 3545 (2000).

[35] H. Ray and A. C. Roy, Phys. Rev. A **46,** 5714 (1992).

[36] A. Lahmam-Bennani, A. Naja, E. M. Staicu Casagrande, N. Okumus, C. Dal Cappello, I. Charpentier and S. Houamer, J. Phys. B **42,** 165201 (2009).

[37] E. O. Steinborn and E. Filter, *Translations of Fields Represented by Spherical-Harmonic Expansions for Molecular Calculations*, Theoret. Chim. Acta (Berl.) **38**, 247 (1975).

[38] M. Abramowitz and I. A. Stegun, Handbook of mathematical functions (Dover, New York) (1972).

Figure captions

Figure 1a: Triple differential cross section for 250eV electron-impact ionization of the $2a_1$ orbital of the water. The theoretical calculation is performed in the first Born approximation (L=0 partial wave contribution).The energy of the ejected electron is E_e=10 eV and the scattered angle is 15^0.

Figure 1b: (Color online) Triple differential cross section for 250eV electron-impact ionization of the $2a_1$ orbital of the water. The theoretical calculation is performed in the first Born approximation. The energy of the ejected electron is E_e=10 eV and the scattered angle is 15^0. Contribution of L=1 (solid line), of L=2 (dashed line), of L=3 (dotted line), and of L=4 (dash-and-dotted line).

Figure 2a: (Color online) Triple differential cross section for 250eV electron-impact ionization of the $2a_1$ orbital of the water. The energy of the ejected electron is E_e=10 eV and the scattered angle is 15^0. The theoretical calculations are performed in the first Born approximation (solid line), in the second Born approximation (dashed line) and with the eikonal approximation (dotted line). The experimental data are those of Milne-Brownlie *et al*. [3].

Figure 2b: (Color online) Triple differential cross section for 250eV electron-impact and positron-impact ionization of the $2a_1$ orbital of the water. The energy of the ejected electron is E_e=10 eV and the scattered angle is 15^0.

The theoretical calculations are performed in the first Born approximation (solid line) and in the second Born approximation for electron impact (dashed line) and for positron impact (dotted line).

Figure 3a: (Color online) Summed triple differential cross section for 250eV electron-impact ionization of the $1b_1$ and $3a_1$ orbitals of the water. The energy of the ejected electron is respectively E_e=10 eV for the $1b_1$ orbital and 8 eV for the $3a_1$ orbital. The scattered angle is 15^0.

The theoretical calculations are performed in the first Born approximation (solid line) and in the second Born approximation (dashed line). The experimental data are those of Milne-Brownlie *et al*. [3].

Figure 3b: (Color online) Summed triple differential cross section for 250eV electron-impact ionization of the $1b_1$ and $3a_1$ orbitals of the water. The energy of the ejected electron is respectively E_e=10 eV for the $1b_1$ orbital and 8 eV for the $3a_1$ orbital. The scattered angle is 15^0.

The theoretical calculations are performed in the first Born approximation (solid line) and in the second Born approximation for electron impact (dashed line) and for positron impact (dotted line).

Figure 4a: (Color online) Triple differential cross section for 250eV electron-impact ionization of the $1b_1$ orbital of the water. The energy of the ejected electron is E_e=10 eV and the scattered angle is 15^0.

The theoretical calculations are performed in the first Born approximation (solid line) and in the second Born approximation (dashed line). The experimental data are those of Milne-Brownlie *et al*. [3].

Figure 4b: (Color online) Triple differential cross section for 250eV electron-impact and positron-impact ionization of the $1b_1$ orbital of the water. The energy of the ejected electron is E_e=10 eV and the scattered angle is 15^0.

The theoretical calculations are performed in the first Born approximation (solid line) and in the second Born approximation for electron impact (dashed line) and for positron impact (dotted line).

Figure 5a: (Color online) Triple differential cross section for 250eV electron-impact ionization of the $1b_2$ orbital of the water. The energy of the ejected electron is E_e=10 eV and the scattered angle is 15^0. The theoretical calculations are performed in the first Born approximation (solid line) and in the second Born approximation (dashed line). The experimental data are those of Milne-Brownlie *et al*. [3].

Figure 5b: (Color online) Triple differential cross section for 250eV electron-impact and positron-impact ionization of the $1b_2$ orbital of the water. The energy of the ejected electron is E_e=10 eV and the scattered angle is 15^0.

The theoretical calculations are performed in the first Born approximation (solid line) and in the second Born approximation for electron impact (dashed line) and for positron impact (dotted line).

Figure 6a: (Color online) Triple differential cross section for 250eV electron-impact ionization of the first valence orbital of the thymine (ionization energy: I_i=9.14 eV). The energy of the ejected electron is E_e=20 eV and the scattered angle is 15^0.

The theoretical calculations are performed in the first Born approximation: partial wave L=1 (thin solid line), partial waves L=1 to L=2 (dashed line), partial waves L=1 to L=3 (dotted line), partial waves L=1 to L=4 (dash and dotted line), partial waves L=1 to L=5 (dash-dot dotted line), partial waves L=1 to L=6 (short dashed line),and partial waves L=1 to L=10 (thick solid line).

Figure 6b: (Color online) Triple differential cross section for 250eV electron-impact ionization of the first valence orbital of the thymine (ionization energy: I_i=9.14 eV). The energy of the ejected electron is E_e=20 eV and the scattered angle is 15^0.

The theoretical calculations are performed in the first Born approximation: partial wave L=1 to L=8 (thick solid line) and partial waves L=1 to L=10 (dashed line).

Figure 7a: (Color online) Triple differential cross section for 250eV electron-impact ionization of the first valence orbital of the thymine (ionization energy: I_i=9.14 eV). The energy of the ejected electron is E_e=20 eV and the scattered angle is 10^0.

The theoretical calculations are performed in the first Born approximation: partial wave L=1 (thin solid line), partial waves L=1 to L=2 (dashed line), partial waves L=1 to L=3 (dotted line), partial waves L=1 to L=4 (dash and dotted line), partial waves L=1 to L=5 (dash-dot dotted line), partial waves L=1 to L=6 (short dashed line),and partial waves L=1 to L=10 (thick solid line).

Figure 7b: (Color online) Triple differential cross section for 250eV electron-impact ionization of the first valence orbital of the thymine (ionization energy: I_i=9.14 eV). The energy of the ejected electron is E_e=20 eV and the scattered angle is 10^0.

The theoretical calculations are performed in the first Born approximation: partial wave L=1 to L=8 (thick solid line) and partial waves L=1 to L=10 (dashed line).

Figure 8a: (Color online) Triple differential cross section for 250eV electron-impact ionization of the second valence orbital of the thymine (ionization energy: I_i =11eV). The energy of the ejected electron is E_e=20 eV and the scattered angle is 15^0.

The theoretical calculations are performed in the first Born approximation: partial wave L=1 (thin solid line), partial waves L=1 to L=2 (dashed line), partial waves L=1 to L=3 (dotted line), partial waves L=1 to L=4 (dash and dotted line), partial waves L=1 to L=5 (dash-dot dotted line), partial waves L=1 to L=6 (short dashed line),and partial waves L=1 to L=10 (thick solid line).

Figure 8b: (Color online) Triple differential cross section for 250eV electron-impact ionization of the second valence orbital of the thymine (ionization energy: I_i=11eV). The energy of the ejected electron is E_e=20 eV and the scattered angle is 15^0.

The theoretical calculations are performed in the first Born approximation: partial wave L=1 to L=8 (thick solid line) and partial waves L=1 to L=10 (dashed line).

Figure 9a: (Color online) Triple differential cross section for 250eV electron-impact ionization of the second valence orbital of the thymine (ionization energy: I_i=11eV). The energy of the ejected electron is E_e=20 eV and the scattered angle is 10^0.

The theoretical calculations are performed in the first Born approximation: partial wave L=1 (thin solid line), partial waves L=1 to L=2 (dashed line), partial waves L=1 to L=3 (dotted line), partial waves L=1 to L=4 (dash and dotted line), partial waves L=1 to L=5 (dash-dot dotted line), partial waves L=1 to L=6 (short dashed line),and partial waves L=1 to L=10 (thick solid line).

Figure 9b: (Color online) Triple differential cross section for 250eV electron-impact ionization of the second valence orbital of the thymine (ionization energy: I_i=11eV). The energy of the ejected electron is E_e=20 eV and the scattered angle is 10^0.

The theoretical calculations are performed in the first Born approximation: partial wave L=1 to L=8 (thick solid line) and partial waves L=1 to L=10 (dashed line).

Figure 10a: (Color online) Triple differential cross section for 250eV electron-impact ionization of the third valence orbital of the thymine (ionization energy: I_i=11.4eV). The energy of the ejected electron is E_e=20 eV and the scattered angle is 15^0.

The theoretical calculations are performed in the first Born approximation: partial wave L=0 (thin solid line), partial waves L=0 to L=1 (dashed line), partial waves L=0 to L=2 (dotted line), partial waves L=0 to L=3 (dash and dotted line), partial waves L=0 to L=4 (dash-dot dotted line), partial waves L=0 to L=5 (short dashed line),and partial waves L=0 to L=6 (short dotted line) and partial waves L=0 to L=10 (thick solid line).

Figure 10b: (Color online) Triple differential cross section for 250eV electron-impact ionization of the third valence orbital of the thymine (ionization energy: I_i=11.4eV). The energy of the ejected electron is E_e=20 eV and the scattered angle is 15^0.

The theoretical calculations are performed in the first Born approximation: partial wave L=0 to L=8 (solid line), partial waves L=0 to L=9 (dashed line) and partial waves L=0 to L=10 (dotted line).

Figure 11a: (Color online) Triple differential cross section for 250eV electron-impact ionization of the third valence orbital of the thymine (ionization energy: I_i=11.4eV). The energy of the ejected electron is E_e=20 eV and the scattered angle is 10^0.

The theoretical calculations are performed in the first Born approximation: partial wave L=0 (thin solid line), partial waves L=0 to L=1 (dashed line), partial waves L=0 to L=2 (dotted line), partial waves L=0 to L=3 (dash and dotted line), partial waves L=0 to L=4 (dash-dot dotted line), partial waves L=0 to L=5 (short dashed line),and partial waves L=0 to L=6 (short dotted line) and partial waves L=0 to L=10 (thick solid line).

Figure 11b: (Color online) Triple differential cross section for 250eV electron-impact ionization of the third valence orbital of the thymine (ionization energy: I_i=11.4eV). The energy of the ejected electron is E_e=20 eV and the scattered angle is 10^0.

The theoretical calculations are performed in the first Born approximation: partial wave L=0 to L=8 (solid line), partial waves L=0 to L=9 (dashed line) and partial waves L=0 to L=10 (dotted line).

Figure 12a: (Color online) Triple differential cross section for 250eV electron-impact ionization of the fourth valence orbital of the thymine (ionization energy: I_i=12.16eV). The energy of the ejected electron is E_e=20 eV and the scattered angle is 15^0.

The theoretical calculations are performed in the first Born approximation: partial wave L=0 (thin solid line), partial waves L=0 to L=1 (dashed line), partial waves L=0 to L=2 (dotted line), partial

waves L=0 to L=3 (dash and dotted line), partial waves L=0 to L=4 (dash-dot dotted line), partial waves L=0 to L=5 (short dashed line),and partial waves L=0 to L=6 (short dotted line) and partial waves L=0 to L=10 (thick solid line).

Figure 12b: (Color online) Triple differential cross section for 250eV electron-impact ionization of the fourth valence orbital of the thymine (ionization energy: I_i=12.16eV). The energy of the ejected electron is E_e=20 eV and the scattered angle is 15^0.
The theoretical calculations are performed in the first Born approximation: partial wave L=0 to L=10 (solid line), partial waves L=0 to L=12 (dashed line) and partial waves L=0 to L=30 (dotted line).

Figure 13a: (Color online) Triple differential cross section for 250eV electron-impact ionization of the fourth valence orbital of the thymine (ionization energy: I_i=12.16eV). The energy of the ejected electron is E_e=20 eV and the scattered angle is 10^0.
The theoretical calculations are performed in the first Born approximation: partial wave L=0 (thin solid line), partial waves L=0 to L=1 (dashed line), partial waves L=0 to L=2 (dotted line), partial waves L=0 to L=3 (dash and dotted line), partial waves L=0 to L=4 (dash-dot dotted line), partial waves L=0 to L=5 (short dashed line) and partial waves L=0 to L=6 (short dotted line) and partial waves L=0 to L=10 (thick solid line).

Figure 13b: (Color online) Triple differential cross section for 250eV electron-impact ionization of the fourth valence orbital of the thymine (ionization energy: I_i=12.16eV). The energy of the ejected electron is E_e=20 eV and the scattered angle is 10^0.
The theoretical calculations are performed in the first Born approximation: partial wave L=0 to L=8 (solid line), partial waves L=0 to L=9 (dashed line) and partial waves L=0 to L=10 (dotted line).

Figure 14: (Color online) Triple differential cross section for 250eV electron-impact and positron-impact ionization of the first valence orbital of the thymine (ionization energy: I_i=9.14 eV). The energy of the ejected electron is E_e=20 eV and the scattered angle is 10^0.

The theoretical calculations are performed in the first Born approximation (solid line) and in the second Born approximation for electron impact (dashed line) and for positron impact (dotted line).

Figure 1a

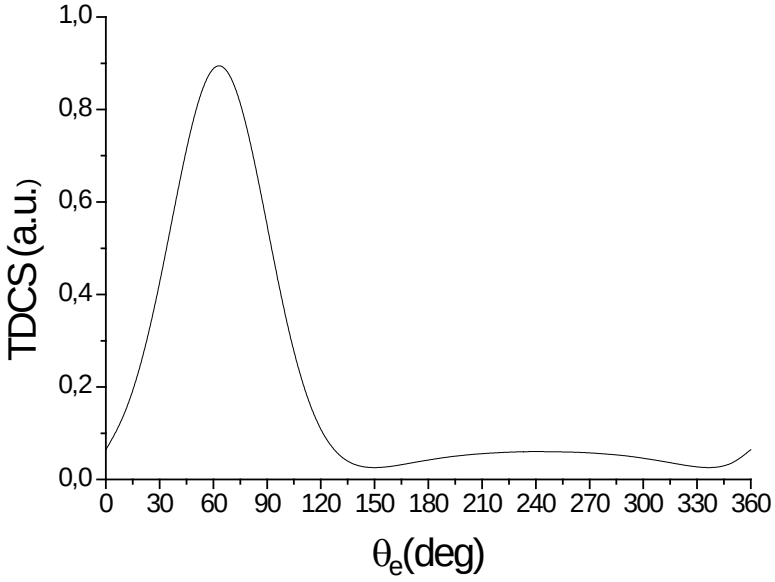

Figure 1b

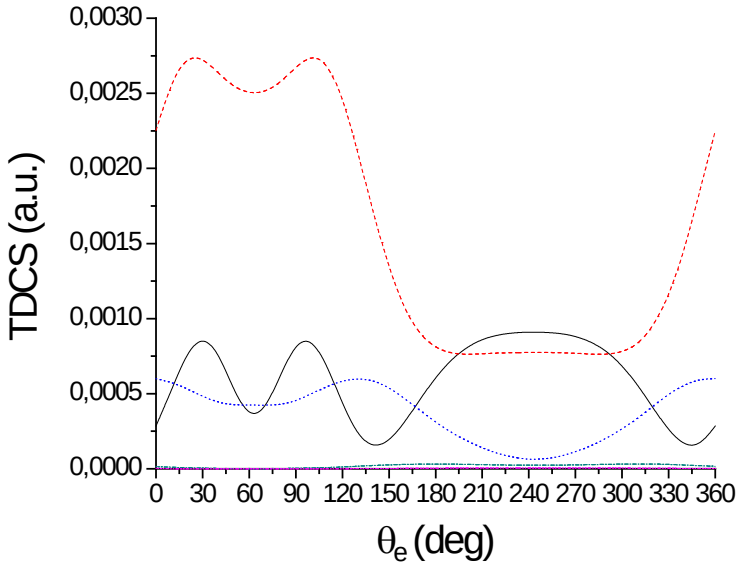

Figure 2a

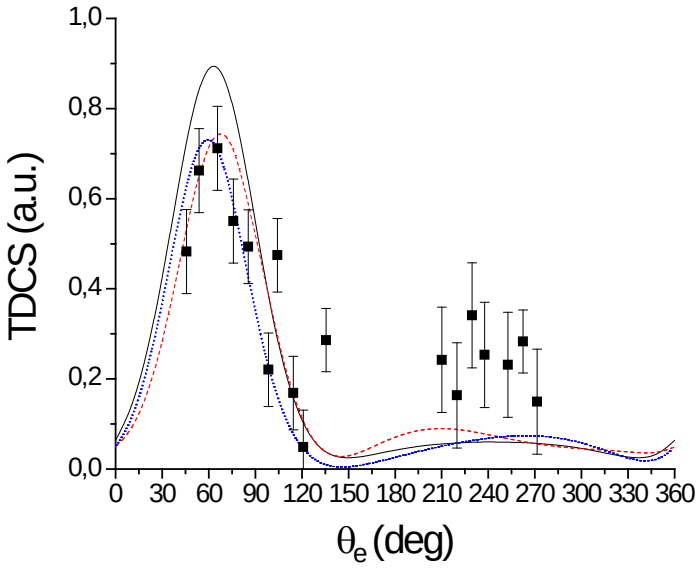

Figure 2b

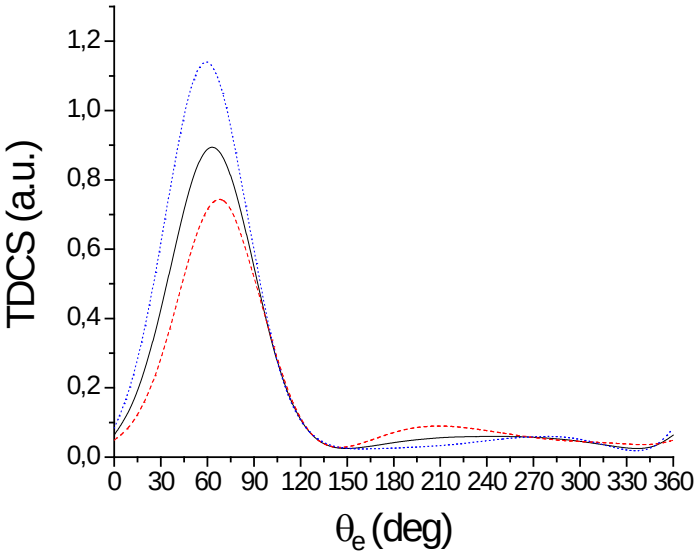

Figure 3a

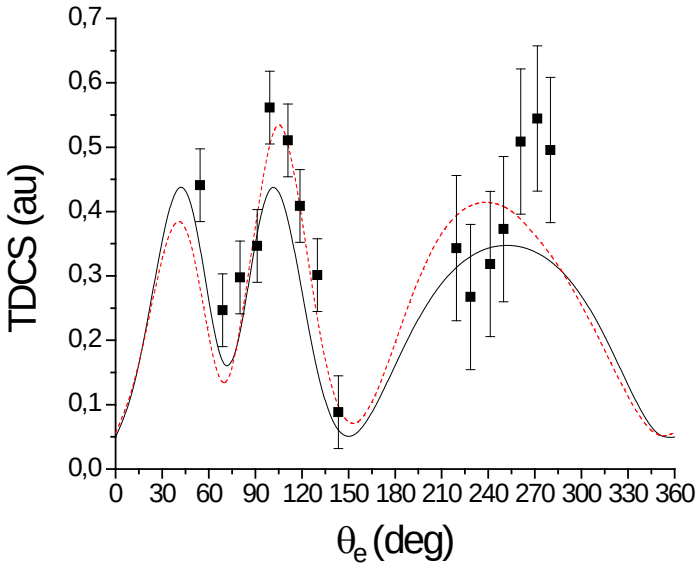

Figure 3b

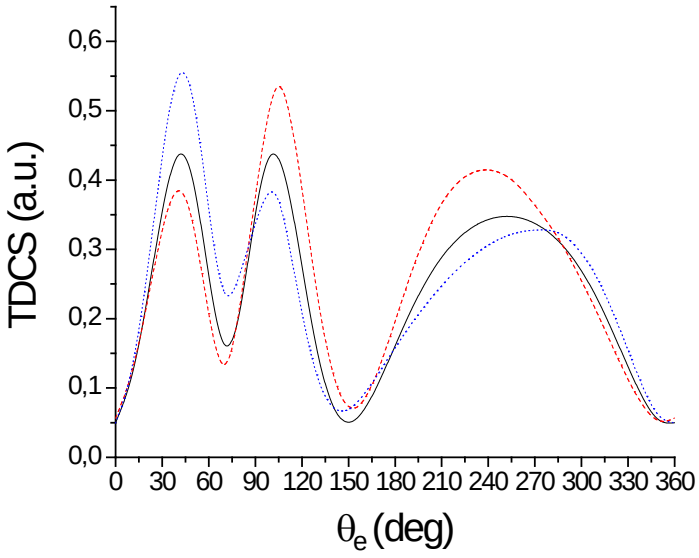

Figure 4a

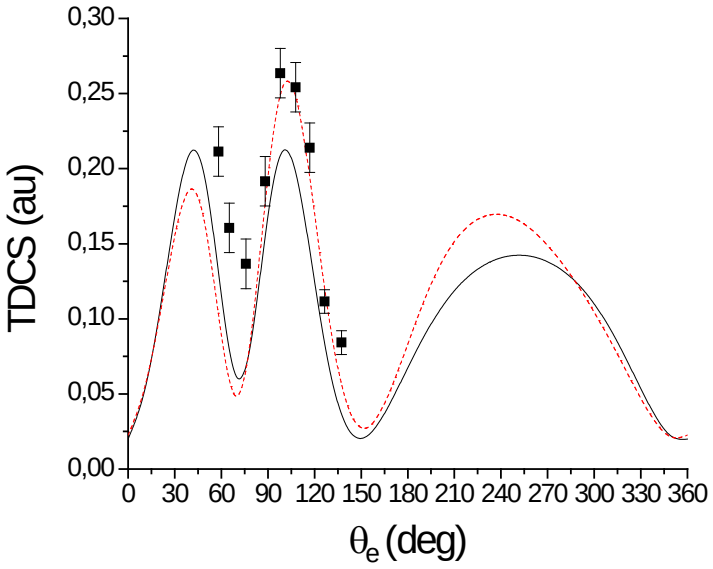

Figure 4b

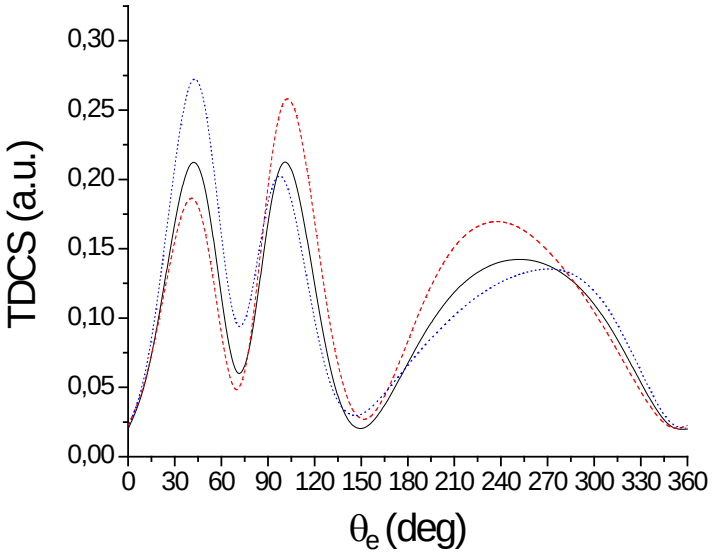

Figure 5a

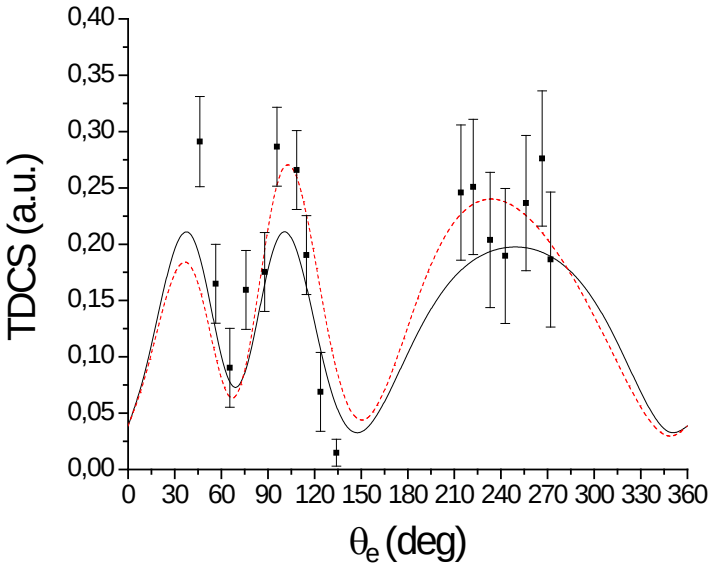

Figure 5b

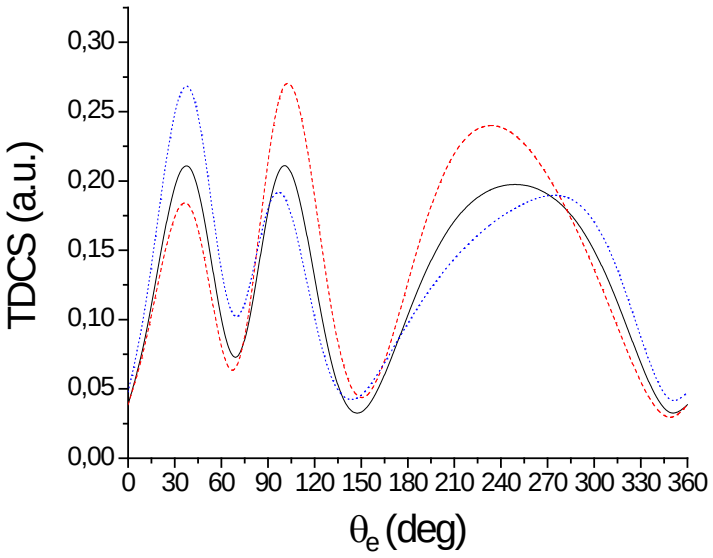

Figure 6a

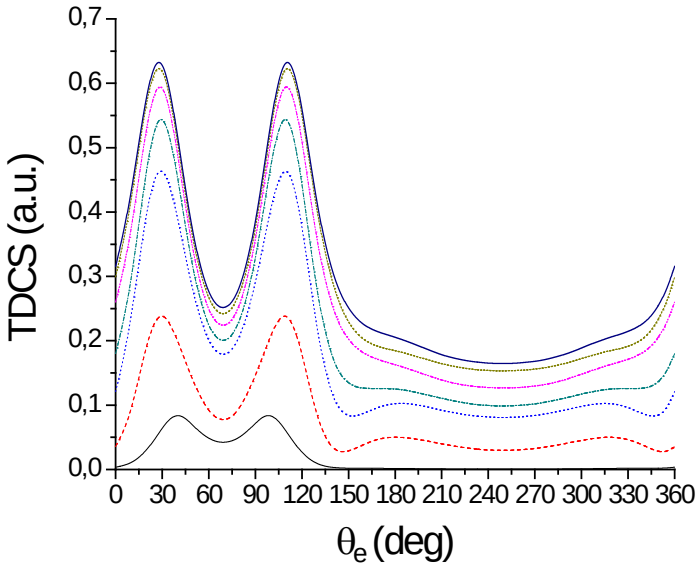

Figure 6b

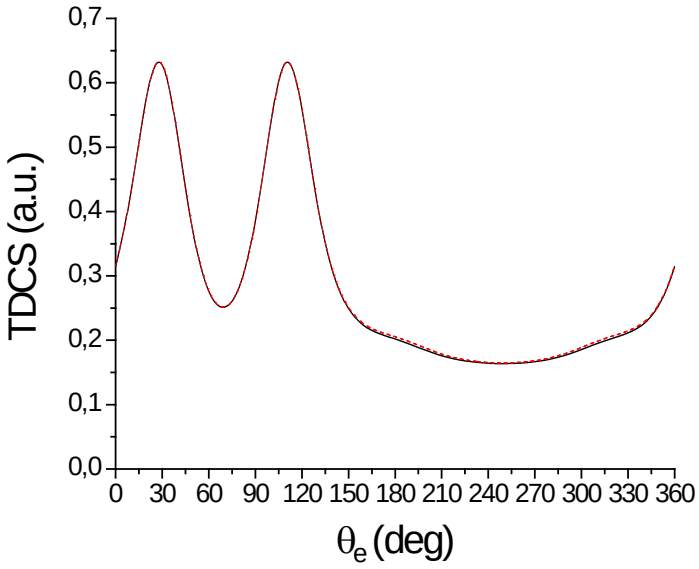

Figure 7a

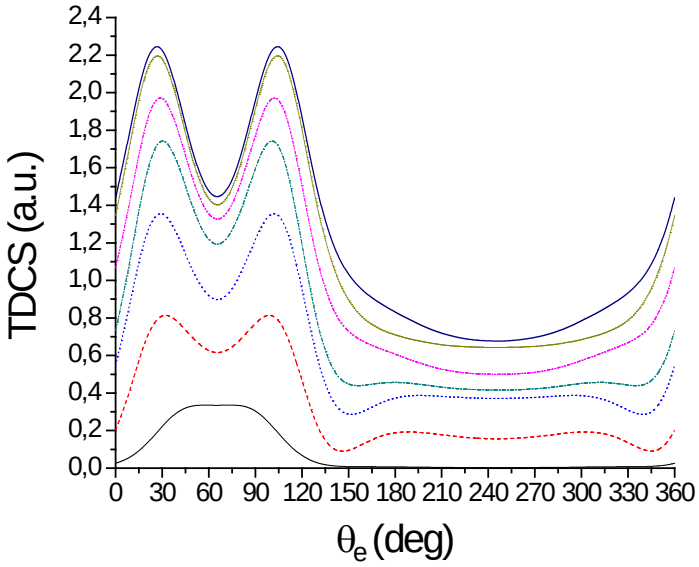

Figure 7b

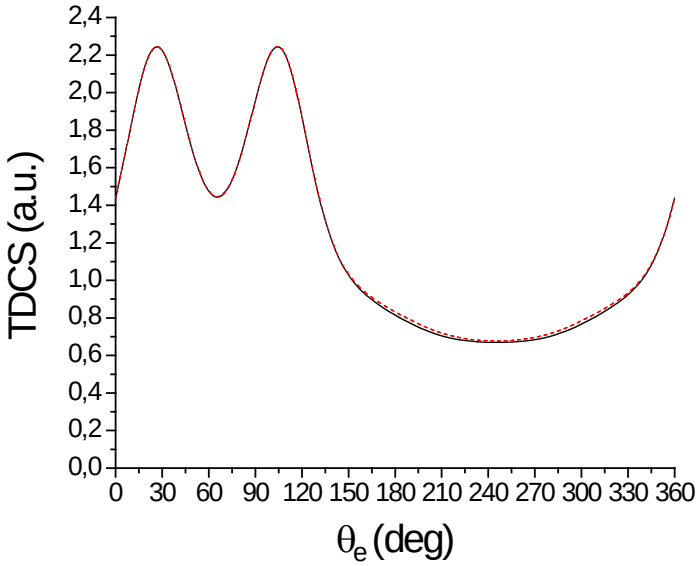

Figure 8a

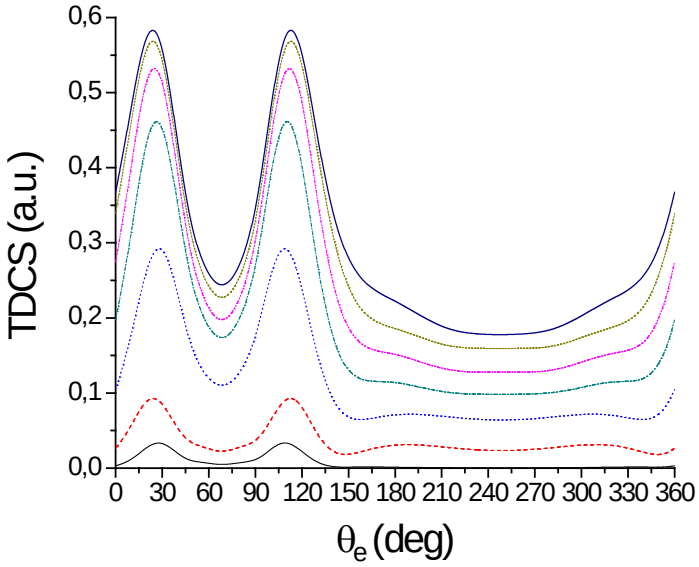

Figure 8b

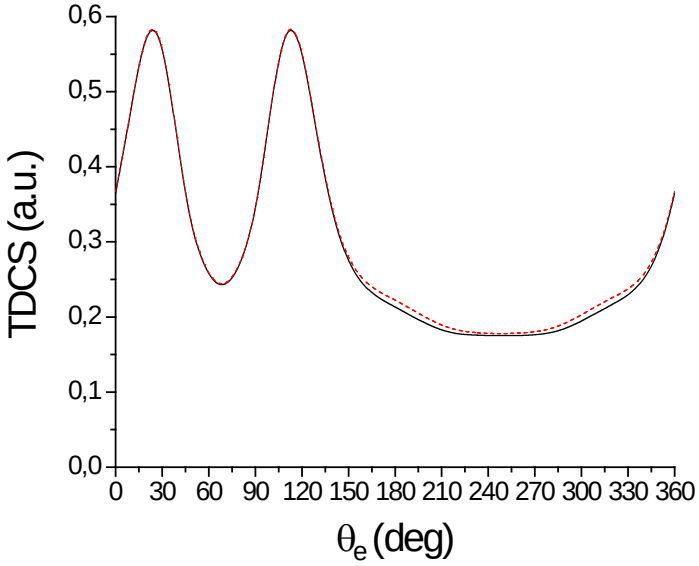

Figure 9a

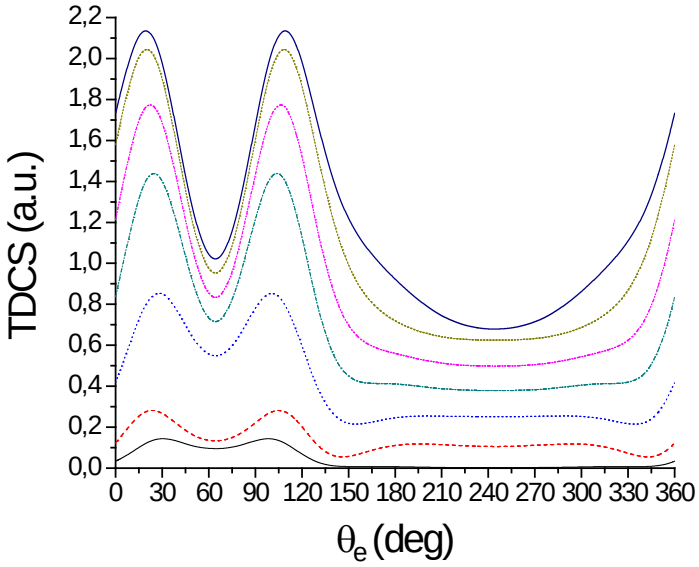

Figure 9b

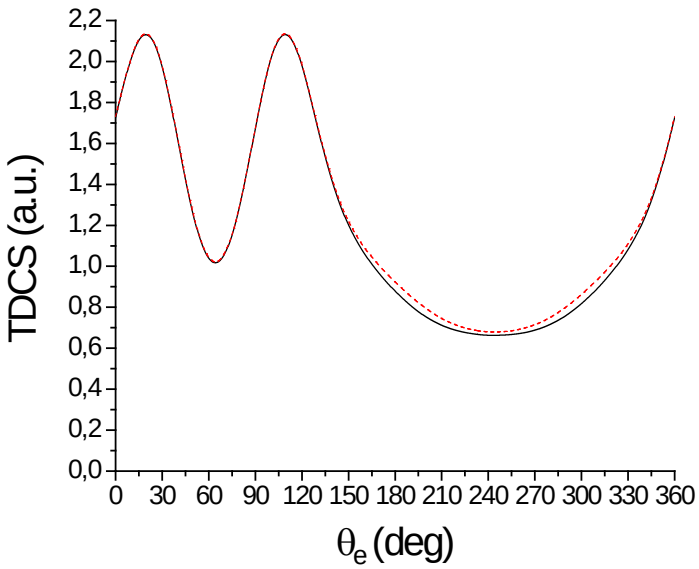

Figure 10a

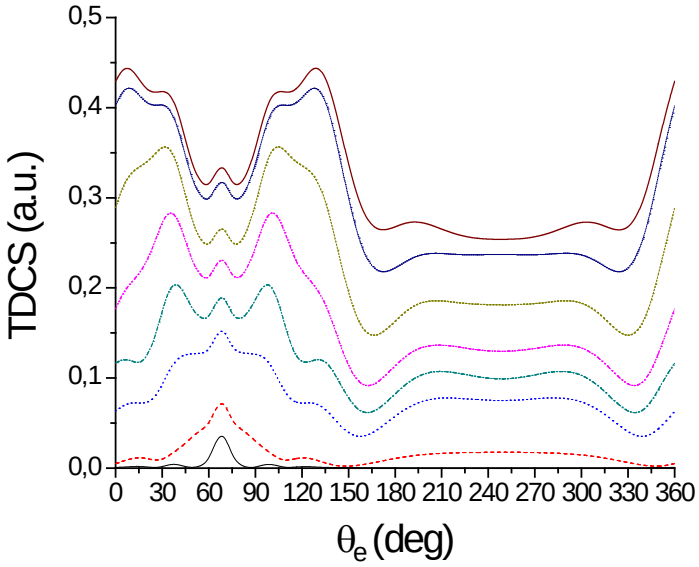

Figure 10b

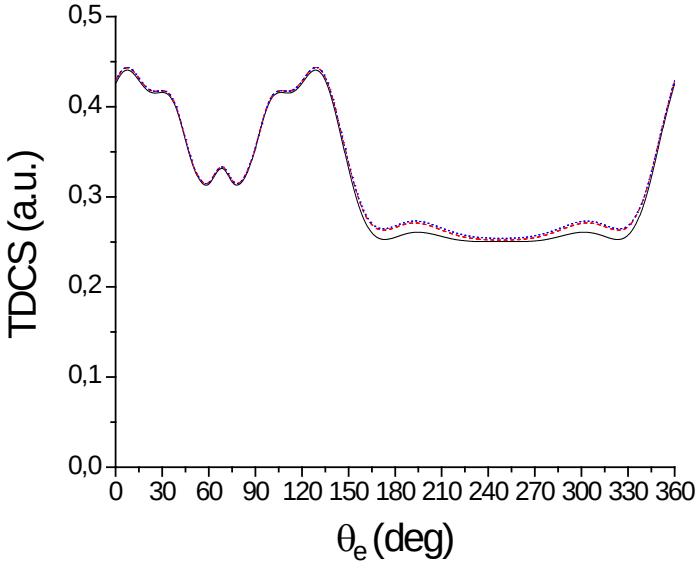

Figure 11a

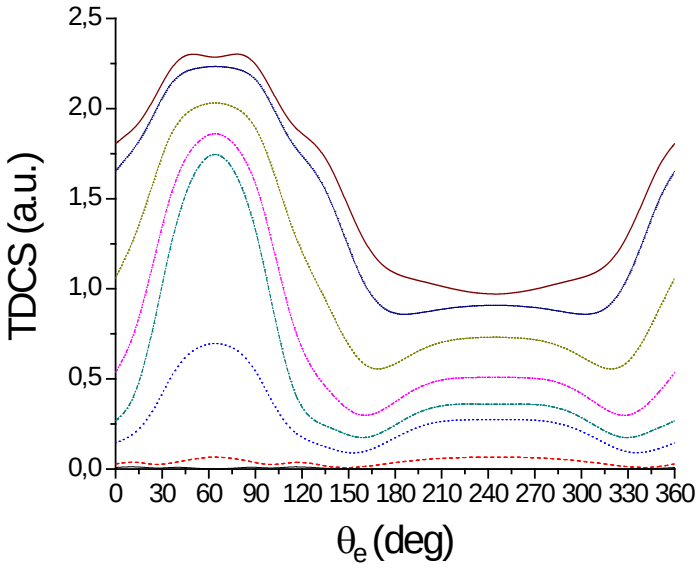

Figure 11b

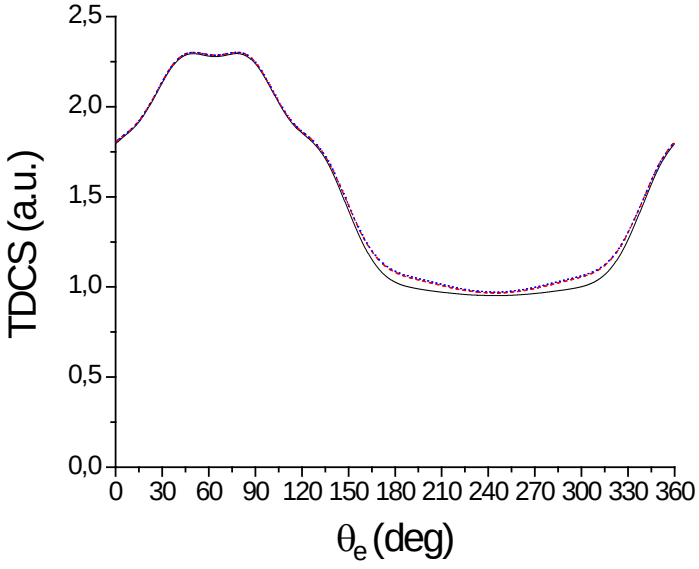

Figure 12a

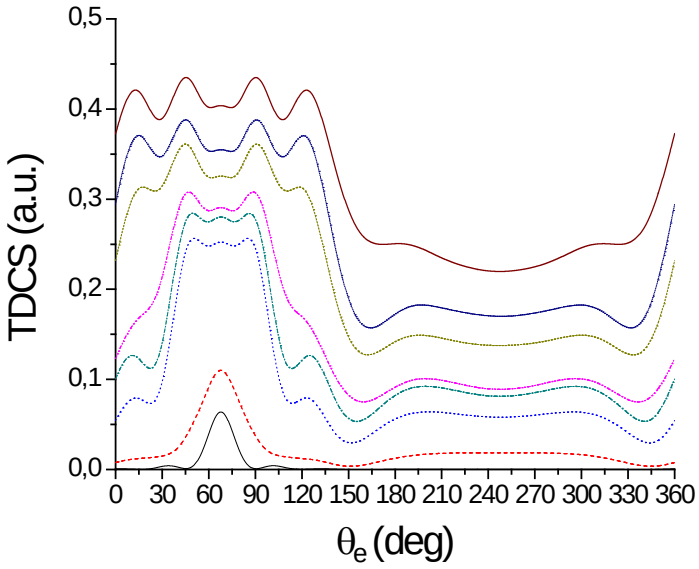

Figure 12b

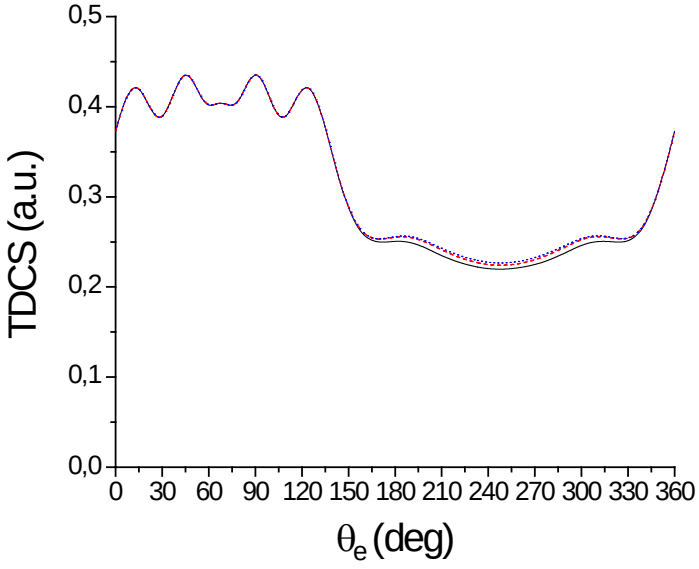

Figure 13a

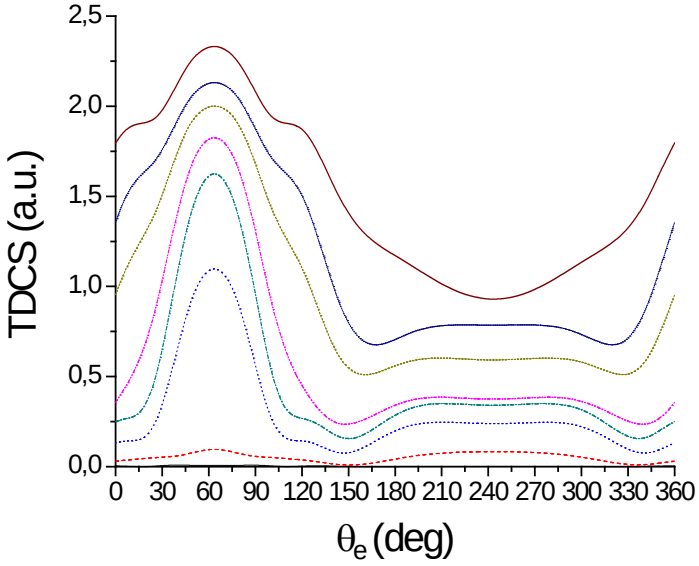

Figure 13b

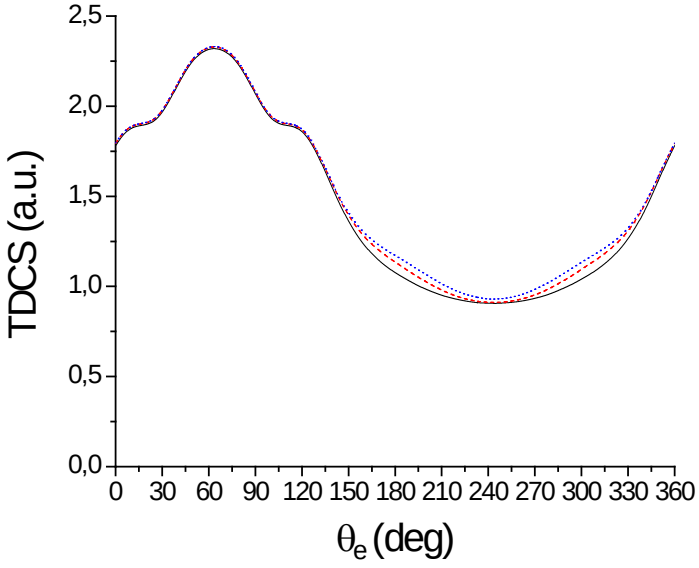

Figure 14

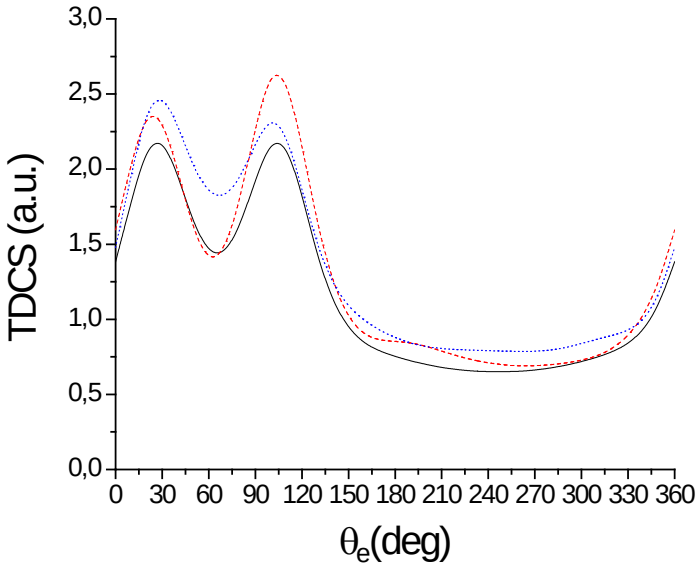
TDCS (a.u.)
3,0
2,5
2,0
1,5
1,0
0,5
0,0
0 30 60 90 120 150 180 210 240 270 300 330 360
θe(deg)